Long baseline imaging with LOFAR

Javier Moldón and Eskil Varenius

1 Introduction

The prime reason to include the international LOFAR stations in the array is to obtain very high-resolution images. Using the longest LOFAR baselines, subarcsecond imaging is possible with High Band Array (HBA) and the upper part of the Low Band Array (LBA). Early science results include images of AGN jets, and of individual supernova remnants in M82 (see Fig. 1). In this chapter we describe the international LOFAR stations and, in general terms, some important things to keep in mind when observing, calibrating and imaging data including *long* baselines, i.e. baselines to international stations. In particular we summarise how techniques from Very Long Baseline Interferometry (VLBI) can be used to calibrate LOFAR data using the longest baselines. Some parts of the text are focused on HBA data; calibration and imaging of long baseline data from the LBA is more challenging and additional work is still needed to find the best approach.

1.1 The international LOFAR stations

The majority of the LOFAR stations, namely the core and remote stations, are distributed over an area roughly 180 km in diameter predominantly in the northeastern Dutch province of Drenthe. Currently, the array also includes 9 international LOFAR stations across Europe that provide maximum baselines up to 1292 km. Three additional stations are under construction in Poland, extending the maximum

Javier Moldón
ASTRON, Postbus 2, 7990 AA Dwingeloo, The Netherlands, e-mail: moldon@astron.nl

Eskil Varenius
Onsala Space Observatory, Dept. of Earth and Space Sciences, Chalmers University of Technology, SE-43992 Onsala, Sweden e-mail: varenius@chalmers.se

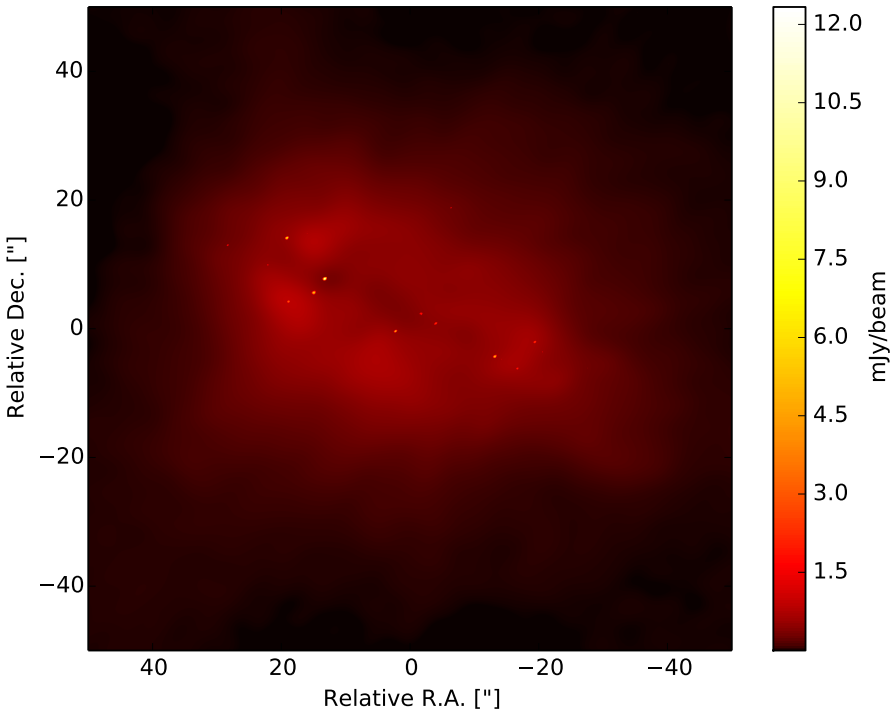

Fig. 1 Combined high resolution and low resolution image of M82 illustrating the relative brightness between the compact and extended emission at 154 MHz. The synthesized beam size of the International LOFAR image is $0.36'' \times 0.23''$ and has an rms noise level of 0.15 mJy/beam. (Varenius et al. 2015)

baseline to ∼2000 km. Fig. 2 shows the distribution of stations already existing or currently in construction.

1.2 Sampling of Fourier space

The core stations provide maximum baselines of 2.7 km, the remote stations of 120 km, and the international stations of 1300 km. Table 1 shows the distances between each pair of international stations, including the core station CS001 as a reference to the center of the array. Since there are relatively few international stations, the sampling of Fourier space (*uv*-coverage) is less dense for baselines to international stations compared to core- and remote baselines. A typical LOFAR *uv* coverage is shown in Fig. 3. It should be noted that because of the wide bandwidth offered by LOFAR, Multi-Frequency-Synthesis techniques can be used in imaging to provide very good *uv*-coverage also at the longest baselines.

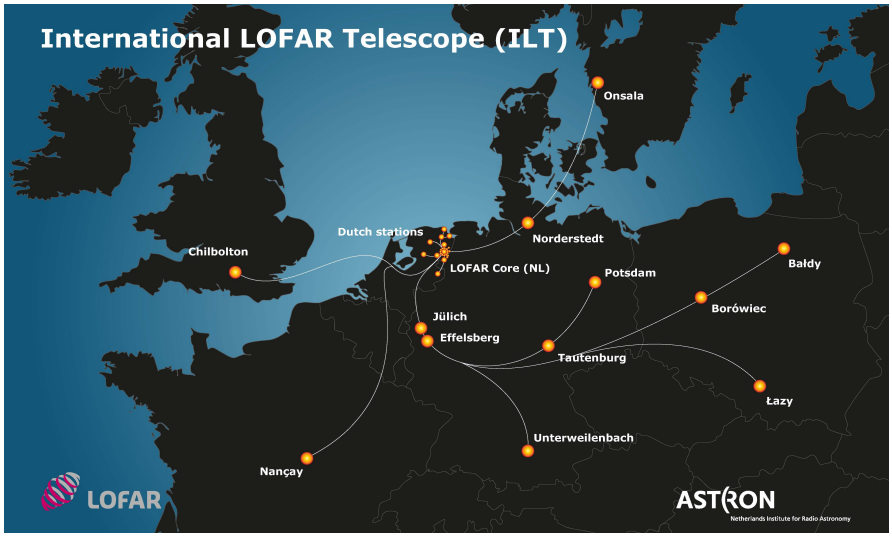

Fig. 2 LOFAR is composed by 24 core stations and 13 remote stations in the Netherlands, and 9 international stations (+3 under construction).

	CS001	DE601	DE602	DE603	DE604	DE605	FR606	SE607	UK608
CS001	0	266	581	396	419	226	700	594	602
DE601	266	0	390	344	476	53	490	833	590
DE602	581	390	0	277	455	440	690	990	959
DE603	396	344	277	0	186	372	800	714	920
DE604	419	476	455	186	0	487	957	556	1005
DE605	226	53	440	372	487	0	498	807	552
FR606	700	490	690	800	957	498	0	1292	495
SE607	594	833	990	714	556	807	1292	0	1110
UK608	602	590	959	920	1005	552	495	1110	0

Table 1 Separation in km between the Dutch core and the currently available international stations.

1.3 Resolution and sensitivity

In general, the image resolution from interferometric data depends on the sampling of fourier space and relative weighting applied to the visibilities when imaging. A quick estimate can however be obtained using the well known expression $\theta \approx \lambda/D$ where λ is the wavelength of observation, D is the maximum baseline length, and θ is the angular resolution in radians. For international LOFAR baselines we estimate an angular resolution of about 0.3" at 150 MHz. This is also verified in practice, for example in the observations of M82 Varenius et al. (2015). Estimates for LBA and HBA can be found in Table 2.

The expected image noise depends on many factors, such as which baselines to include in the final imaging, but also on the solar activity at the time of observa-

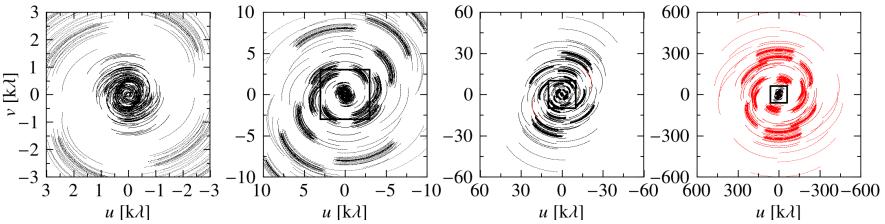

Fig. 3 *uv* coverage for a 4-hr observation of a source at declination $+48^\circ$ with a single subband centred at 140 MHz. Only one visibility every 160 seconds is shown. The rectangles in the last three panels show the area covered by the previous panel. Visibilities corresponding to baselines with international stations are plotted in red.

tion. For subarcsecond imaging it is common to exclude the NL-baselines and only include data on baselines to international stations. LOFAR HBA is most sensitive at frequencies around 150 MHz (van Haarlem et al. 2013, Fig. 22). Varenius et al. (2015) obtained rms noise levels of 0.3 mJy/beam at 118 MHz and 0.15 mJy/beam at 154 MHz using 16 MHz bandwidth and 16 hours of integration, in reasonable agreement with theoretical estimates (see Varenius et al. (2015) for a brief discussion on the expected thermal noise). Since then, more international stations have became available and station calibration has been improved. It is reasonable to assume similar rms noise levels (scaling with bandwidth and intergration time) can be expected in future observations using international baselines.

1.4 Field of view

The sky area possible to image from any LOFAR observation is limited by factors such as the station beam, baseline projection effects, and atmospheric disturbances across the sky. NL-LOFAR observations are often also limited by very bright interfering sources, such as the *A-team*. International baseline imaging is in many aspects simpler than Dutch baseline imaging, because we can generally ignore interference from other bright sources in the sky.

For a distant potentially interfering source, the interfering contribution to the target source visibility declines by factors of u^{-1} as a function of baseline length (u) for both frequency and time decorrelation (also called *smearing*. Furthermore, for most of the source population resolved on longer Dutch LOFAR baselines, the intrinsic visibility structure decreases faster than u^{-2} (a rough approximation based on experience of typical dependence of visibility amplitude vs baseline length for resolved radio sources), giving a total decrease of interfering signals with baseline length scaling as u^{-4}. This means that the effect of interfering signals is a million times less for baselines of 1000 km as opposed to 30 km. This effect explains why the influence of the brightest sources at LOFAR frequencies, like Cassiopeia A or

Cygnus A, can be ignored at international baseline resolution, as can most Jansky level sources within the station beam.

For very high-resolution imaging we are often interested in specific objects covering a small part of the sky. This small field of view regime is where cm-VLBI usually operates and this regime greatly simplifies imaging. In this regime, target images are generally smaller than the isoplanatic patch, and therefore only a single-direction station-dependent correction needs to be determined. Likewise, over such small fields, *w*-term effects and station beam variations can generally be ignored. This is different from LOFAR core-resolution imaging, where in order to get noise-limited (rather than "dynamic range"-limited) images at any given point in a field the whole field must be imaged using multi-directional calibration techniques.

Whether one can produce useful images using the small-field approximation and VLBI software depends on the brightness of the target source and, if necessary, the availability of close sources to use as calibrators similar to what is done in cm-VLBI.

1.4.1 Time and frequency smearing

Although smearing helps to simplify calibration by reducing the influence of bright interfering sources, care has to be taken to not average too much so that the science targets are affected. In this section we estimate the impact of smearing on the field of view.

For LOFAR, the standard *raw* data are delivered from the correlator with resolution 1 second in time, and 64 channels per subband. Each subband (using the standard 200 MHz clock) is 195 kHz wide, meaning that the default minimum averaging bandwidth is 3 kHz. This will limit the dynamic range at some distance from the observed phase center, similar to the limit imposed by the station beam. A detailed description of the averaging losses is beyond the scope of this chapter, we merely quote the often used results by Taylor et al. (1999) chapter 18, who derived two expressions to estimate the average amplitude loss due to averaging in frequency and time, at some distance from the phase center. For frequency smearing, we can use their expression 18-24 assuming a square bandpass and circular Gaussian tapering, where the reduction in amplitude at a distance from the phase centre r can be estimated as

$$\frac{I}{I_0} = \frac{\sqrt{\pi}}{2\sqrt{\ln 2}} \frac{\theta \nu_c}{r \Delta \nu} \mathrm{erf}\left(\sqrt{\ln 2} \frac{r \Delta \nu}{\theta \nu_c} \right) \tag{1}$$

where θ is the synthesized beam size (FWHM), ν_c is the central frequency of the observation, and $\Delta\nu$ is the bandwidth. Note that the units of θ and r cancel if they are given in the same unit. Note also that this expression is in fact independent of central frequency ν_c since the synthesised beam also scales with ν_c, only the bandwidth is important.

For time smearing, we may use their formula 18-43, assuming a 12 hour average over a circular UV-coverage with Gaussian tapering:

$$\frac{I}{I_0} = 1 - 1.22 \times 10^{-9} \left(\frac{r}{\theta}\right)^2 \Delta t^2 \quad (2)$$

where Δt is the averaging time in seconds.

What loss to define as acceptable of course depends on your science, in particular the brightness of your target, but as a general guide one may tolerate 5% loss in amplitude due to averaging. Using the standard LOFAR raw data values, we have calculated the corresponding circle (diameter, to compare with station FWHM) for different observing frequencies, see Table 2. We have also included estimates for a typical long baseline observation averaging to 2s and 4ch/subband.

Freq. (MHz)	λ (m)	Int. PSF FWHM ($''$)	Int. station FHWM (deg)	5% loss, 1s Diam. (deg)	5% loss, 64ch/SB Diam. (deg)	5% loss, 2s Diam. (deg)	5% loss, 4ch/SB Diam. (deg)
15	19.99	2.54	19.39	9.02	3.30	4.51	0.21
30	9.99	1.27	9.70	4.51	3.30	2.26	0.21
45	6.66	0.85	6.46	3.01	3.30	1.50	0.21
60	5.00	0.63	4.85	2.26	3.30	1.13	0.21
75	4.00	0.51	3.88	1.80	3.30	0.90	0.21
120	2.50	0.32	2.59	1.13	3.30	0.56	0.21
150	2.00	0.25	2.07	0.90	3.30	0.45	0.21
180	1.67	0.21	1.73	0.75	3.30	0.38	0.21
200	1.50	0.19	1.55	0.68	3.30	0.34	0.21
210	1.43	0.18	1.48	0.64	3.30	0.32	0.21
240	1.25	0.16	1.29	0.56	3.30	0.28	0.21

Table 2 Station FWHM Values taken from (van Haarlem et al. 2013, App. B). Loss due to time- and frequency averaging as calculated using equations 2 and 1 assuming a 1300 km baseline. Note that the expression given for frequency smearing is independent of observing frequency, only the channel bandwidth is important.

2 Calibration of international LOFAR stations

In this section we describe, in general terms, how to calibrate phase and amplitudes of visibilites on baselines to international stations. More detailed information can be found in the LOFAR imaging cookbook.

2.1 Phase calibration using international stations

Accurate phase calibration of the visibilities for a weak (or unknown) target source is usually done by finding residual phase errors using a calibrator (point-like or with a good model) close to the target source, and then transferring the derived corrections to the target. In principle, phase corrections can be determined separately for

each channel if the data has high enough signal-to-noise. In practice, the requirement of a nearby calibrator often means that the calibrator too weak, and therefore necessary to average in time and/or frequency to gain sufficient SNR to find the desired phase corrections. This can however only be done if there is no residual delay (causing a change of phase with respect to frequency) or rate (causing a change of phase with respect to time) present in the data. Unfortunately, residual delays and rates are common on international baselines, and we have to deal with them to be able to correct residual phase errors before imaging. Below we first describe the origin and timescales to be expected for delays and rates in LOFAR HBA data. Then we discuss how to use VLBI self-calibration techniques (i.e. fringe-fitting) to remove desidual rates and delays from the data.

2.1.1 Residual delays and rates

The phase of a single visibility depends on the time delay of the signal to reach two different stations. A given time delay will cause different phase-errors for different observing frequencies. We define the phase delay as $\tau_\phi = \phi/2\pi\nu$. We clearly see that a delay between two stations will produce a phase slope as funtion of frequency, which is also visible in the data, see e.g. Fig. 4(a).

Residual delays can arise due to multiple effects which are not accurately modeled in the LOFAR correlator, for example:

- Errors in station positions or target source positions
- Instrumental effects (e.g. atomic clock drifts)
- Propagation through the ionosphere.

If the model applied during correlation were perfect, all stations would see a delay offset of zero for an isolated compact source, but deviations are produced by several factors.

Errors in station positions (and currently at a much lower level errors in the the Earth orientation parameters) produce residual delays on the order of 75 ns, varying with a 24 h periodicity. These errors can be expected to be greatly reduced in the near future. Errors in the *a priori* centroid position (for example from low-frequency catalogues, with a typical error of a few arcseconds) and/or extended structure on subarcsecond scales, introduce an additional delay. The maximum baseline between an international station and the LOFAR core (the correlator reference point) is 700 km (see Table 1); a positional error of $1.5''$ will lead to a residual delay of $\sim$15 ns on this baseline.

Instabilities in the rubidium clocks used at the international stations (the core stations share a single clock) can produce delay rates up to 20 ns per 20 min, which corresponds to about a radian per minute at 150 MHz (van Haarlem et al. 2013). In total, non-dispersive delays of up to $\sim$ 100 ns and delay rates of up to $\sim$20 ns h^{-1} are expected.

The ionospheric contribution to the delay changes as a function of time, position, and zenith angle. The magnitude of the changes depend on the Total Electron

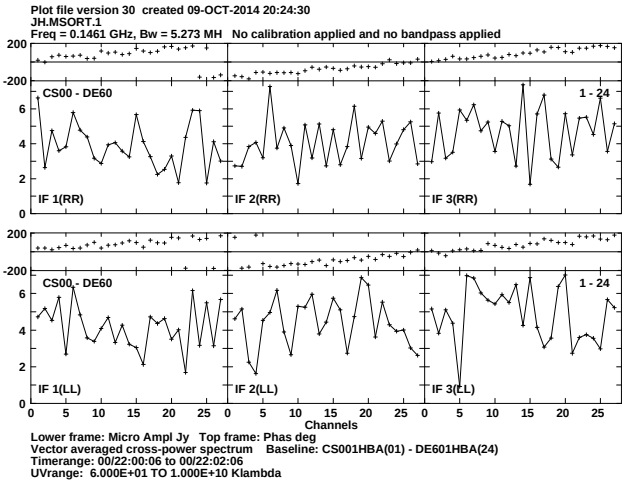

(a) Before fringe fitting

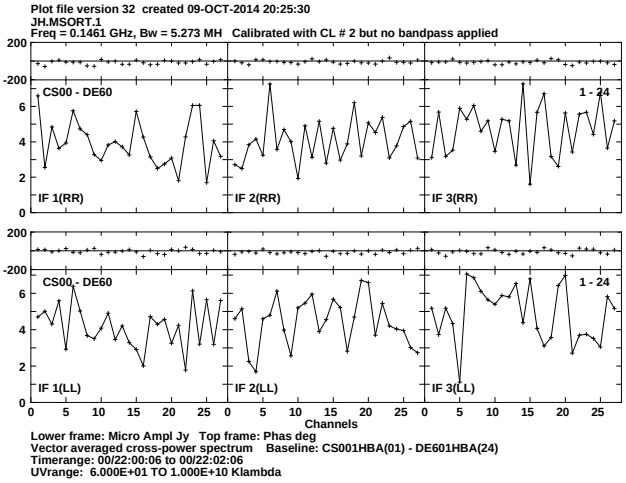

(b) After fringe fitting

Fig. 4 Two figures showing the effect of fringe fitting on two minutes of data on the baseline CS001HBA - DE601HBA for source J0958+6533 in project LC0_26. Both polarisations are shown, and the data are divided in three spectral windows (IFs in AIPS) of 5.3 MHz each. After applying the corrections from FRING, the phase is flat with respect to frequency, see (b), as it should be for a point source.

Content (TEC) of the ionosphere, with a delay of $\tau_{\rm ion} = c^2 r_{\rm e}/(2\pi\nu^2) \times {\rm TEC}$, being c the speed of light, $r_{\rm e}$ the classical electron radius, and ν the observed frequency. The TEC, usually measured in TEC Units (1TECU $= 10^{16}$ electrons m^{-2}), can be estimated using models derived from observations of GPS satellites. The models contain information on the vertical total electron content (VTEC) during an observations. We note that the TEC values above the stations are a lower limit of the slant ionospheric contribution that depends on the source elevation at each station. More details can be found in, for instance, Nigl et al. (2007) and Sotomayor-Beltran et al. (2013).

Although the VTEC follows a 24-h trend strongly correlated with the Sun elevation, the short-term (10–60 minute) variations between the widely separated international stations are virtually uncorrelated. The ionospheric contribution typically dominates the total delay and delay rate for international LOFAR stations. Even after a complete phase calibration, the residual ionospheric delays between the calibrator and the target source can be important. We have used VLBI observations (VLBA project code BD152) at 300 MHz, or 1 m wavelength, of bright and compact pulsars at different angular separations to obtain a rough estimate of the delay difference between sources separated 1–5 degrees at elevations of 50–80°. As a first approximation we estimated that the dispersive delay difference between sources at different lines of sight should be about 5 ns per degree of separation, for a source elevation of 60°.

Finally, the determination of the delays will be limited by the brightness of the source used to calibrate them, and the sensitivity of the station. In summary, in a normal observation phase uncertainties are caused by source position and structure errors, differential ionosphere, uncorrected instrumental delays, and noise. Table 3 summarises the main contributions and the time scale in which they change.

Table 3 Approximate delay contributions at 140 MHz to a 700 km baseline.

Effect	Delay	Time scale
Non-Dispersive		
Correlator model error	$\sim$ 75 ns	24h (periodic)
Station clocks	$\sim$ 20 ns	$\sim$20 min
Source position offset (1.5″)	$\sim$ 15 ns	–
Dispersive		
Slowly varying ionosphere	$\sim$ 300 ns	$\sim$hours
Rapidly varying ionosphere	$\gtrsim$10 ns	$\sim$ 10 min
Differential ionosphere (source elevation 60 deg)	5 ns/deg sep.	–

2.1.2 Correcting residual delays and rates

Due to the large and time-variable delay offsets at each station, solving for phase corrections directly (approximating the correction as constant over a given solu-

tion time and bandwidth) would require very narrow solution intervals for VLBI, and hence an extremely bright calibrator source ($\gtrsim$ 10 Jy). However, such a source would be unlikely to be close on the sky to the target. With a separation of perhaps tens of degrees the differential atmosphere/ionosphere between the calibrator and the target direction would render the derived calibration useless in the target direction. We can make use of fainter calibrators closer to the target with the VLBI phase calibrator known as *fringe-fitting*: simultaneously solving for 3 parameters (phase, non-dispersive delay, and phase rate) in each solution interval, allowing the solution duration and bandwidth to be greatly extended. This technique is very similar to ordinary phase calibration, but in addition to solving for phase we solve for a phase change with respect to frequency (delay) and time (rate).

Currently, fringe-fitting (globally) solving for delays and rates is not available within common LOFAR software or in CASA. The current best approach is to use the task *FRING* available within the Astronomical Image Processing System (AIPS[1]) (Greisen 2003). This task can however only solve for a *linear* change of phase with respect to frequency and time, i.e. a non-dispersive delay and constant rate within a specific solution interval.

Two options present themselves: to add additional parameters (covering dispersive delay and dispersive delay rate) to the global fit, or to reduce the solution bandwidth such that the constant dispersive delay approximation becomes valid again. The former option is obviously preferable from a sensitivity perspective, but greatly expands and complicates the solution search space. Efforts are underway to implement such an expanded fit, including in addition differential Faraday rotation, which becomes increasingly important at frequencies below 100 MHz. First tests on individual long baselines of LOFAR as well as baselines to other telescopes are promising, but the algorithms are not yet sufficiently mature for public use. Accordingly, we focus here on sources which can serve as primary calibrators under the latter set of conditions, where solution bandwidths are limited to no more than a few MHz and time intervals of a few minutes.

2.1.3 What is a bright enough calibrator?

To derive delay and rate corrections we need to find a calibrator which is bright enough to find solutions in a small enough block in time and frequency so that the linear approximation is valid. The system equivalent flux density (SEFD) of a single LOFAR core station is approximately 1500 Jy[2] at a frequency of $\sim$140 MHz (van Haarlem et al. 2013). An international station has twice the collecting area of a core station at $\sim$140 MHz, so the expected SEFD is around 750 Jy. The theoretical 1σ baseline sensitivity of an international station to a (joined) HBA core station, given 3 MHz of bandwidth and 4 minutes of observing time, is 40 mJy in a single

[1] http://www.aips.nrao.edu/index.shtml

[2] A LOFAR core station consists of two sub-stations (2×24 tiles) in the HBA.

polarisation. If we require a minimum signal to noise ratio of 5 for fringe-fitting, this means we need a calibrator brighter than 200 mJy.

It is possible to use even weaker calibrators by forming a combined station of all the core stations, resulting in a very sensitive station wieh an SEFD of $\sim$65 Jy (see Sect. 4.2). The theoretical 1σ baseline sensitivity of an international station to the phased-up core station, given 3 MHz of bandwidth and 4 minutes of observing time, is hence 8 mJy in a single polarisation. Given this increase in sensitivity, sources with flux densities as low as 50 mJy could in theory be used as delay/rate calibrators. However, in practice the sensitivity may be reduced by failing tiles, imperfect station calibration and correlated (astronomical) noise. Also, solution intervals shorter than 4 minutes could be required under suboptimal ionospheric conditions. Therefore, 50 mJy should be considered a lower limit for a useful delay/rate calibrator flux density.

2.1.4 What is a close enough calibrator?

In addition to being sufficiently bright, the delay/rate calibrator must be close enough to the target field that the differential delay between the two fields does not lead to decorrelation when phase-only secondary calibration is performed (as done for cm VLBI, either using the target itself or using another calibrator). The solution bandwidths are narrower by a factor of $\gtrsim$10 than for cm VLBI, which is helpful, but the ionospheric delay (inversely proportional to observing frequency squared) is much greater, meaning that on balance a calibrator closer than the $\lesssim$5 degrees typical for cm VLBI will be needed. The maximum acceptable separation will be a strong function of ionospheric conditions and elevation, but at face value, given a bandwidth 20 times narrower (e.g., 3 MHz vs 64 MHz) and frequency 10 times lower (140 MHz vs 1400 MHz), one would expect that the calibrator would typically need to be separated by $\lesssim$1 degree. This is borne out by commissioning observations with LOFAR, which have shown acceptable results with separations up to several degrees in favourable ionospheric conditions, and unacceptable results with separations as small as $\sim$0.8 degrees in poor conditions. Ideally, then, a primary calibrator for International LOFAR observations would be located $\lesssim$1 degree from the secondary calibrator/target field to give acceptable calibration under most circumstances. Exploration of the distribution of compact sources at 140 MHz has shown that the density of calibrators on the sky could be enough to overcome this restriction (Moldón et al. 2015). This leads to the one calibration advantage of International LOFAR compared to cm VLBI; since the beam of an International LOFAR station is $\gtrsim$2 degrees across, the calibrator may easily be observed simultaneously with the target source. Note however that care has to be taken when averaging the data to not reduce amplitudes severely by smearing, see Sect. 1.4.1. This can for example be avoided by using the *shift+averaging procedure*, see Sect. 4.1.2.

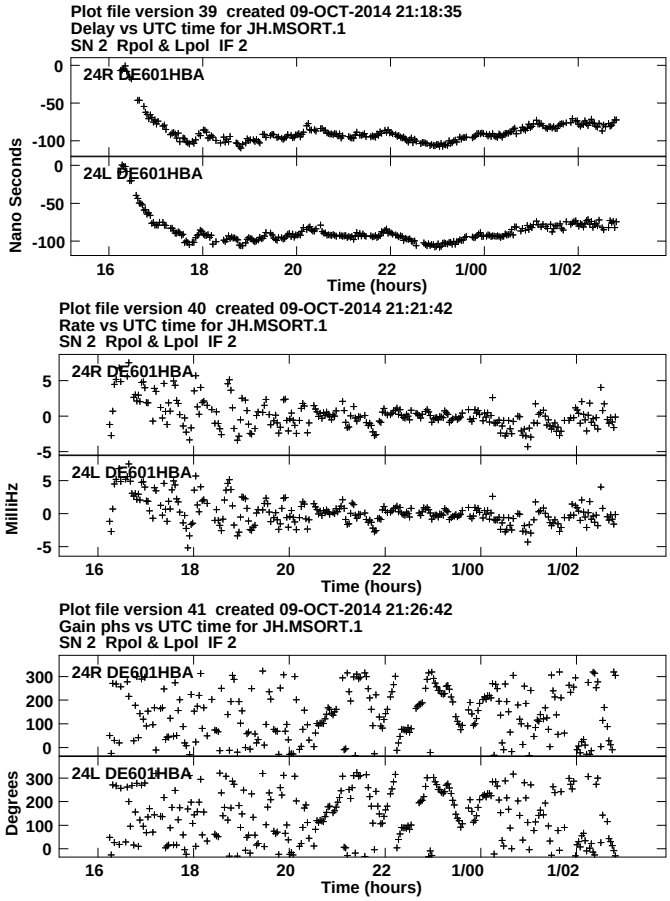

Fig. 5 Delay (top), rate (middle) and phase(bottom) corrections derived for the source J0958+6533 at 154 MHz by FRING for station DE601HBA for right and left circular polarisation. These plots show the corrections derived for a 10 hour observation (the first segment of project LC0_026). It is clear from the rates and phases that phases changes rapidly during the first and last hours of the experiment. The delay solutions are more stable, although there is a large change during the first hour. In general, the ionosphere is more stable during midnight than at sunset or sunrise.

2.2 Amplitude calibration of international stations

In principle, instrumental gains within LOFAR could be tracked with time as done in cm-VLBI (this option is currently being commissioning with the COBALT correlator), but since this option is not yet available we rely on calibrators with known flux density.

For core and remote stations one can use, for example, standard flux density calibrators such as 3C196, or bright sources in low frequency catalogs such as MSSS

(Heald & LOFAR Collaboration 2014). However, for international stations this is in general not possible because of the small spatial scales sampled by baselines to these stations. The bright standard flux calibrators, e.g. 3C196, have a very complex structure at subarcsecond scales. If we had a good model of this structure at our frequency of observation, we could account for it in the calibration of the international stations. Work is being done to map well known flux density calibrators with high enough resolution, but until these models are available we have to rely on another boot-strapping technique.

The current best approach is to include two calibrators in the observations: a well monitored flux density calibrator (for instance 3C196 or 3C84) and another compact source with flux density of a few hundred mJy. The compact calibrator can often be the same as used to derive delay/rate solutions, see Sect, 2.1.3. While this compact source can be variable (on timescales longer than the observation), and hence not a suitable *absolute* flux density reference, it can be used to calibrate the *relative* amplitudes of all baselines, including international stations. The absolute flux density scale can then be set by fitting a common scaling factor for all visibilities (including the international baselines), by comparing the derived flux density for the standard flux density calibrator on short (NL) baselines, where subarcsecond scale structure is not important.

After a phase and amplitude calibration of an International LOFAR observation, the resulting visibilities should look similar to the ones shown in Fig. 6, where we show the calibrator J0958+6533 used in Varenius et al. (2015) to derive delay and rate corrections as well as the relative amplitude scale.

3 Observing strategy

Moldón et al. (2015) proposed the following approach for an International LOFAR observation:

1. Identify candidate primary calibrators up to separations of a few degrees by using any of the criteria discussed in Sect. 5.3 in Moldón et al. (2015);
2. Conduct a short observation in snapshot mode as described in Sect. 3.2 before the science observation to identify the best primary calibrator (or calibrators).
3. If required and time permits, follow up with a "full bandwidth" snapshot observation to identify one or more secondary calibrators;
4. Set up the scientific observation to dwell on the field containing the primary calibrator and the target/secondary calibrator;
5. Include periodic scans (every $\sim$ hour) on a bright Dutch array calibrator to calibrate the core stations in order to form the tied station.
6. Shift phase centre to primary calibrator, preprocess and obtain delay solutions as described in this paper, apply them to the unshifted dataset;
7. If a secondary calibrator is to be used and is not yet identified, select 10 minutes of data and perform shift/averaging to candidate secondary calibrator sources;

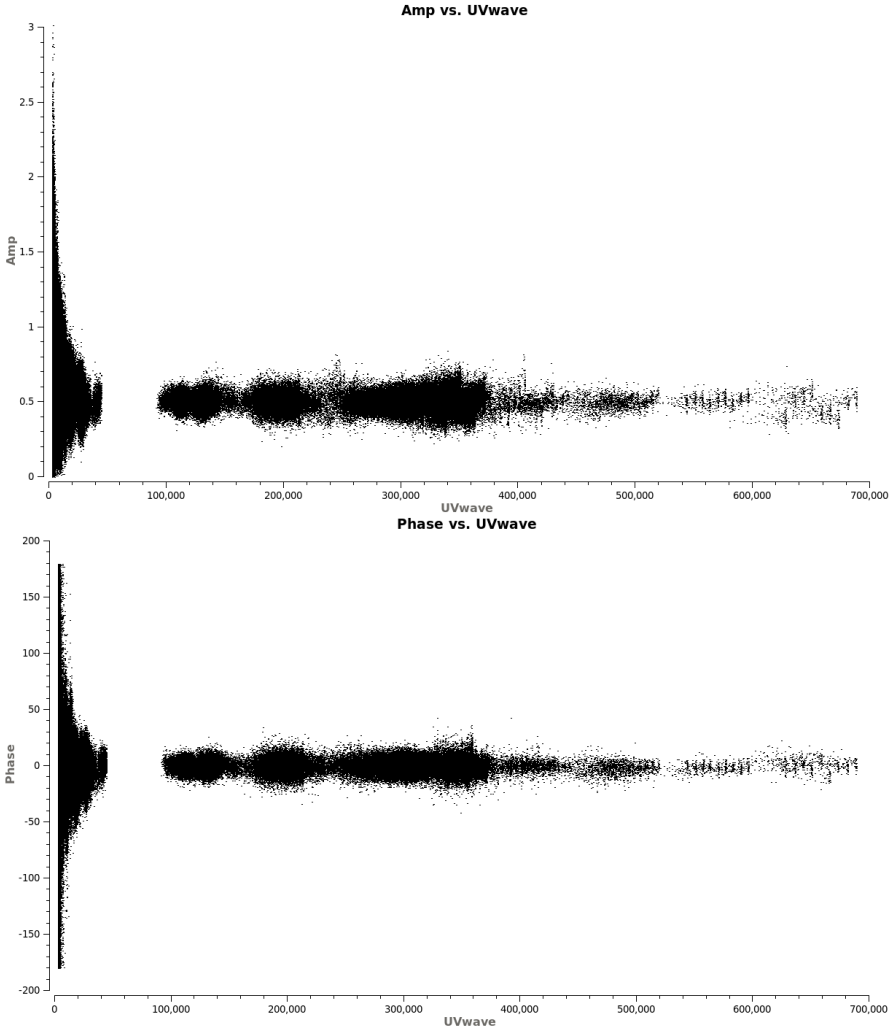

Fig. 6 Amplitude (top) and phase (bottom) vs *uv* distance for a calibrated dataset of J0958+6533. This calibrator has a very compact component of 0.5 Jy, mainly unresolved with the longest LOFAR baselines. We can see how the shorter baselines are sensitive to a much more complex structure and possibly other sources in the field.

8. If secondary calibrator is used: shift and average primary-calibrated dataset, image and selfcalibrate, apply solutions to the unshifted dataset;
9. Shift and average calibrated dataset, image and (if needed) selfcalibrate target.

In the near future, the pipeline used for this project will be developed, in collaboration with the LOFAR operations team, into an expanded form capable of carrying out the approach described above. This pipeline will be made available to all International LOFAR observers, delivering a reduced data volume for long-baseline observations and enabling calibrated data to be more quickly produced.

3.1 Using two calibrators

For cm VLBI, the dispersive delay due to the ionosphere is small (and so are the changes with time), meaning that solution intervals of minutes and widths of tens to hundreds of MHz are generally permissible. After application of the solutions from the primary calibrator it is common to use a secondary calibrator[3] closer to the target source (separation $\sim$arcmin), or to use the target source if it is bright enough for "self-calibration", solving only for the phase (no delay or rate). This second phase-only calibration is used to refine the calibration errors that result from the spatial or temporal interpolation of the primary solutions. Because this is a problem with fewer degrees of freedom, lower signal-to-noise ratio (S/N) data can be used. Additionally, because the bulk delay has already been removed, even more bandwidth can be combined in a single solution for a further improvement in S/N. A secondary calibrator can therefore be considerably fainter (usually $\sim$1-10 mJy versus $>$100 mJy for a primary calibrator). This typical VLBI calibration strategy is illustrated in Figure 7.

3.2 Finding calibrators

Until a good catalogue of compact sources at MHz frequencies is available, it is important to take into account that a science observation might require a preparatory search of calibrators. A fast method using the distribution of bandwidth between many sources (see Sect. 4.1) is described in Moldón et al. (2015). A preselection based on a number of parameters from existing catalogues, such as the low-frequency spectral index, and the flux, ca be performed to optimize the search. In particular the most useful catalogues are the VLSS, at 74 MHz, 4 m wavelength (Lane et al. 2012), the WENSS catalogue at 325 MHz, 92 cm wavelength (Rengelink et al. 1997), and specially The Multifrequency Snapshot Sky Survey (MSSS), which comes from LOFAR observations (Heald & LOFAR Collaboration 2014).

[3] A secondary calibrator is often referred to as an "in-beam" calibrator in VLBI if it is close enough to the target source to be observed contemporaneously

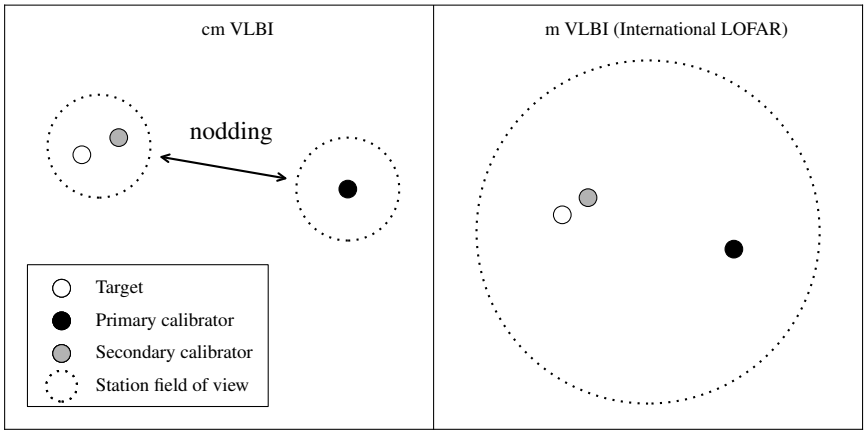

Fig. 7 Typical calibration setup for cm VLBI (left) and International LOFAR (right). Note that in some cases the target may itself function as the secondary calibrator. A secondary calibrator is not always required for cm VLBI, but will almost always be needed for International LOFAR, unless the primary calibrator is fortuitously close. The larger field of view of LOFAR means that both the primary and secondary calibrators will always be observed contemporaneously, unlike in cm VLBI, where nodding between the primary calibrator and target is typically required (shown by the double arrow in the left panel).

Moldón et al. (2015) showed that there is a density of ~ 1 good calibrator per square degree based on two fields with Galactic latitudes of $+26.6^\circ$ and $+43.4^\circ$. However, we expect less compact sources at lower Galactic latitudes due to interstellar scattering. The Galactic electron density model NE2001 (Cordes & Lazio 2002) predicts an scattering at a galactic latitude of 50° of almost 100 mas at 150 MHz, which is five times smaller than our resolution. However, the scattering is about 300 mas, similar to our beamsize, at latitudes of 5–10°, depending on the longitude. Therefore, observations below a Galactic latitude of 10° are likely to be affected by scattering on the longest baselines, and the effect should be severe below about 2°, especially towards the Galactic Center.

4 Practical considerations

4.1 Optimising use of available bandwidth

It is possible to distribute LOFAR bandwidth over a number of beams to simultaneously observe different regions of the sky. In particular, it is possible to divide the bandwidth on target(s) and calibrator, which provides a continuous source calibration without the need of regularly nodding from target to calibrator. Another possibility is to distribute the bandwidth among a large number of sources to search

for suitable calibrators. For example one can generate 30 beams to observe simultaneously 30 sources with 3 MHz bandwith as a fast way to search for suitable compact calibrators for an International LOFAR observation (see i.e. Moldón et al. 2015).

4.1.1 Unequal distribution of subbands on target and calibrators

If your calibrator is bright, you can use fewer subbands on the calibrator, and thereby get better sensitivity on the target. To use fringe finding, we need to sample accurately the residual delay/rate slope (and possibly curvature at low frequencies) present in the data. This can be done with sparse sampling in frequency, where the optimal coverage is achieved by spreading the subbands as a powerlaw density with denser placement of subbands at lower frequencies (Martí-Vidal 2010). The advantage of this approach is that more bandwidth can be placed on the target. The disadvantage is that the calibration becomes a bit more demanding. One reason for this is that the UVFITS format used by AIPS (for running fringe fitting) requires data in all channels. If we do not have contiguous subband coverage in frequency, we need to insert fake data and flag that (e.g. using NDPPP) before reading the data into AIPS. This will cause an increase in data volume which will slow down processing. Also, spreading the subbands sparsely is always a risk in case your calibrator is weaker than you think. A detailed discussion can be found in Martí-Vidal (2010), where the authors analyse how to distribute subbands specifically for LOFAR observations for optimal fringe detection.

4.1.2 The shift + averaging procedure

Given the high resolution obtained with the International LOFAR observations, imaging of the region restricted by the time and frequency average of the data (see Table 2) would require a very high computational cost. If one is interested in multiple objects within the station beam, one can phase-shift (and re-project) the *uv*-data to each object before averaging. After correlation, the full-resolution visibility dataset can be shifted and averaged multiple times, to the positions of all the target sources and possibly to one or more nearby calibrators. Starting in cycle four, it will be possible to request shifting and averaging of data to multiple phase centers within a beam as a part of a normal observation.

4.2 Form a combined station

When studying the very compact structures, the shortest baselines do not add much interesting information but those data slow down the calibration process. The core stations can be added to form a coherent “tied station” (TS001) that keeps the total

core sensitivity on the long baselines to the international stations. Since the core stations are under similar atmospheric conditions and they share the same clock only slow changes in their amplitudes and phases are expected, and thus they can be calibrated by observing a bright primary calibrator once every ~ 1 hr. TS001 can be formed by summing baseline visibilities with the NDPPP task "StationAdder". After this step, all original visibilities with core-core baselines can be discarded using the NDPPP task "Filter" to significantly reduce the data volume.

One important benefit of having a tied station is that it works as a very sensitive station. This tied-array station aids in the derivation of calibration solutions to the international stations with FRING, and can be used as a reference station. We note that a tied-station formed by adding the whole core has a very small (5% amplitude loss at $30''$ distance from phase center) field of view. Although this is rarely a problem for deriving FRING solutions, care is needed if using such combined data to image extended objects.

4.3 Getting LOFAR data into AIPS

The task FRING in AIPS can be used to remove residual delays and rates in the data. However, AIPS requires that the data are in circular polarisation (LOFAR usually stores data in linear polarisation). AIPS also requires the data to be converted from measurement set (MS) to the UVFITS file format. In this section we describe how this can be achieved.

4.3.1 Converting linear to circular polarisation

Differential Faraday rotation introduces rapid phase changes with frequency into linear polarisation data on long baselines. For long-baseline observations is preferable to work in a circular (R,L) polarisation basis. In this basis, the ionospheric disturbances are transformed from coupled amplitude/phase effects (as in the linear X,Y basis) to phase only effects. Since differential Faraday rotation does not mix R and L polarisations we may calibrate RR and LL independently. Furthermore, standard VLBI techniques like fringe fitting work in a circular (R,L) polarisation basis. To run FRING in AIPS, the data have to be converted to circular polarisation.

There are two common ways to convert LOFAR measurement sets to circular polarisation: either using BBS and Table Query Language (TAQL), which uses the BBS beam model, or using the custom software *mscorpol* developed by T. D. Carozzi, which uses its own beam model. Detailed instructions on how to use these tools are provided in the LOFAR Imaging cookbook.

4.3.2 Converting measurement set to UVFITS

Since AIPS understands the UVFITS-format, but not Measurement Sets (MS) we need to convert the data from MS to UVFITS. This can be done using e.g. the tool *ms2uvfits* available at the LOFAR cluster or the task *exportuvfits* in CASA. Note that it is important to have contigous data in frequency (e.g. by filling missing subbands with fake data) and to have data present for all baselines (i.e. by flagging instead of partially filtering antennas).

Acknowledgements This chapter and all the techniques and procedures described in it are based on the work and many useful contributions of the LOFAR long baselines working group. AIPS is produced and maintained by the National Radio Astronomy Observatory, a facility of the National Science Foundation operated under cooperative agreement by Associated Universities, Inc.

References

Cordes, J. M. & Lazio, T. J. W. 2002, ArXiv Astrophysics e-prints
Greisen, E. W. 2003, Information Handling in Astronomy - Historical Vistas, 285, 109
Heald, G. & LOFAR Collaboration. 2014, in American Astronomical Society Meeting Abstracts, Vol. 223, American Astronomical Society Meeting Abstracts #223, 236.07
Lane, W. M., Cotton, W. D., Helmboldt, J. F., & Kassim, N. E. 2012, Radio Science, 47, 0
Martí-Vidal, I. 2010, A&A, 517, A83
Moldón, J., Deller, A. T., Wucknitz, O., et al. 2015, A&A, 574, A73
Nigl, A., Zarka, P., Kuijpers, J., et al. 2007, A&A, 471, 1099
Rengelink, R. B., Tang, Y., de Bruyn, A. G., et al. 1997, A&AS, 124, 259
Sotomayor-Beltran, C., Sobey, C., Hessels, J. W. T., et al. 2013, A&A, 552, A58
Taylor, G. B., Carilli, C. L., & Perley, R. A., eds. 1999, Astronomical Society of the Pacific Conference Series, Vol. 180, Synthesis Imaging in Radio Astronomy II
van Haarlem, M. P., Wise, M. W., Gunst, A. W., et al. 2013, A&A, 556, A2
Varenius, E., Conway, J. E., Martí-Vidal, I., et al. 2015, A&A, 574, A114